World Journal of Orthopedics

Submit a Manuscript: http://www.f6publishing.com

World J Orthop 2017 September 18; 8(9): 660-673

DOI: 10.5312/wjo.v8.i9.660

ISSN 2218-5836 (online)

DIAGNOSTIC ADVANCES

# Clinical applications of advanced magnetic resonance imaging techniques for arthritis evaluation

Teodoro Martín Noguerol, Antonio Luna, Marta Gómez Cabrera, Alexie D Riofrio

Teodoro Martín Noguerol, Antonio Luna, MRI Unit, Clínica Las Nieves, SERCOSA, Health Time, 23007 Jaén, Spain

Antonio Luna, Department of Radiology, University Hospitals of Cleveland, Case Western Reserve University, Cleveland, OH 11100, United States

Marta Gómez Cabrera, MRI Unit, DADISA, Health Time, 11011 Cádiz, Spain

Alexie D Riofrio, Department of Radiology, Duke Regional Hospital, Durham, NC 27710, United States

Author contributions: Martín Noguerol T and Luna A designed this work; Martín Noguerol T and Gómez Cabrera M performed the cases research, Martín Noguerol T, Luna A and Riofrio AD wrote and edited the manuscript.

Conflict-of-interest statement: None.



Manuscript source: Invited manuscript

Correspondence to: Dr. Antonio Luna, Chairman, MRI Unit, Clínica Las Nieves, SERCOSA, Health Time, Carmelo Torres 2, 23007 Jaén, Spain. aluna70@htime.org
Telephone: +34-953-275601
Fax: +34-953-275609

Received: February 11, 2017
Peer-review started: February 15, 2017
First decision: March 27, 2017
Revised: April 26, 2017
Accepted: May 3, 2017
Article in press: May 5, 2017
Published online: September 18, 2017

## Abstract

Magnetic resonance imaging (MRI) has allowed a comprehensive evaluation of articular disease, increasing the detection of early cartilage involvement, bone erosions, and edema in soft tissue and bone marrow compared to other imaging techniques. In the era of functional imaging, new advanced MRI sequences are being successfully applied for articular evaluation in cases of inflammatory, infectious, and degenerative arthropathies. Diffusion weighted imaging, new fat suppression techniques such as DIXON, dynamic contrast enhanced-MRI, and specific T2 mapping cartilage sequences allow a better understanding of the physiopathological processes that underlie these different arthropathies. They provide valuable quantitative information that aids in their differentiation and can be used as potential biomarkers of articular disease course and treatment response.

**Key words:** Magnetic resonance imaging; Joint; Diffusion weighted imaging; Dynamic contrast enhanced; Musculoskeletal system; Cartilage; DIXON; Arthritis



**Core tip:** New magnetic resonance imaging (MRI) techniques, successfully applied in other anatomical areas, can help to improve the diagnostic accuracy for arthritis evaluation. Advanced fat suppression techniques like DIXON or functional sequences such as cartilage imaging, diffusion weighted imaging or dynamic contrast enhanced-MRI are showing promising results for arthritis assessment. These techniques provide both morphological and functional information in several clinical scenarios including infection, degenerative or inflammatory arthritis.

Martín Noguerol T, Luna A, Gómez Cabrera M, Riofrio AD. Clinical applications of advanced magnetic resonance imaging

techniques for arthritis evaluation. *World J Orthop* 2017; 8(9): 660-673 Available from: URL: http://www.wjgnet.com/2218-5836/full/v8/i9/660.htm DOI: http://dx.doi.org/10.5312/wjo.v8.i9.660

## INTRODUCTION

Joint diseases are first evaluated through conventional plain radiography, although this technique is limited in that only late subchondral and bony abnormalities in arthropathies can be detected. Bone scintigraphy has been used to detect the presence of active disease[1]. Ultrasound (US) with Doppler capabilities plays a complementary role in the evaluation of soft tissue involvement for active synovial inflammation assessment without use of radiation or administration of exogenous contrast agents[2]. However, US is limited by operator-dependency and lack of visualization of deep joints. Computed tomography (CT) can help to better define bone involvement in specific joints, particularly when the diagnosis is questionable based on other imaging techniques[3]. A major drawback of CT is its use of ionizing radiation, which limits its use in pediatric population.

The introduction of magnetic resonance imaging (MRI) for joint assessment has overcome several limitations of conventional imaging techniques due to its higher tissue contrast, the ability to obtain multiplanar acquisitions, and the absence of ionizing radiation. Furthermore, MRI sequences permits an early detection of cartilage changes, better depiction of bone and soft tissue edema, and the characterization of synovial involvement[4]. Also, several disease-specific scales based on MRI changes have been proposed to measure arthritis related changes in clinical practice and have been applied in research trials to increase reproducibility[5].

Currently, several new functional MRI techniques have been translated from the brain to the musculoskeletal system which provide physiopathological information of normal tissue and disease. The DIXON sequence allows for very homogeneous fat-suppression in large and small joints, leading to improved detection of bone edema, synovial enhancement, and subchondral involvement. The Dixon sequence also is able to quantitatively define the fat and water content of a tissue, which can be useful in treatment monitoring of arthropathies. Diffusion-weighted imaging (DWI) evaluates the movement of the free water within tissues, allowing for an indirect estimation of cellularity and cell membrane integrity which enables discrimination between hypercellular lesions, such as malignant and inflammatory processes, from normal tissues. DWI can evaluate arthritis in a quantitative manner while avoiding the use of contrast agents.

Dynamic-contrast enhanced MRI (DCE-MRI) exploits differences in tissue vascularization. In this manner, this technique has been used to differentiate the etiology of synovial involvement in arthropathies according to the enhancement pattern and other quantitative derived biomarkers. The use of T2 mapping, which acquires different echo times (TE) within the same sequence, has been shown to aid in the early detection and quantification of cartilage abnormalities based on changes in water content, which indirectly reflects collagen content and collagen fiber orientation in the extracellular matrix. T2 mapping has been primarily used for early detection of osteoarthritis in the knee, as areas of initial cartilage degeneration show longer T2 values.

This review visits the technical basis and quantitative biomarkers provided by all these new advanced MRI techniques in the assessment of arthropathies and succinctly analyze their clinical applications.

## ADVANCED MRI SEQUENCES FOR ARTHRITIS EVALUATION

### *Fat suppression techniques*

The detection of bone edema is considered, along with synovial involvement, as the key feature in assessing joint involvement in arthropathies. The presence of bone edema has been demonstrated to correlate with overall patient outcome, preceding the existence of bone erosions and joint deformity[6,7]. Given its excellent tissue contrast, MRI is considered the single modality able to properly assess the presence, location, and extension of bone edema[8]. Edema imaging is mainly based on fat-suppressed T2-weighted sequences, as the higher water content of involved bone marrow is better depicted against a background of suppressed fat signal. Several sequences have been classically used for evaluation of bone marrow edema, including short inversion time recovery (STIR), spectral presaturation with inversion recovery (SPIR) and spectral adiabatic inversion recovery (SPAIR)[9,10]. Table 1 summarizes the main physical properties of these techniques and their clinical applications.

Bone marrow edema is also well detected on T1-weighted imaging, specifically with chemical shift imaging (CSI). This gradient-echo (GE) based technique exploits the different resonance frequencies of fat and water. In CSI, two different TE are acquired, providing an image where fat signal is subtracted from water signal (opposed-phase image) and another where the signal of water and fat are added (in-phase imaging)[5,6]. CSI has shown potential to differentiate true bone replacement from red bone marrow in different locations, and helps to better identify the presence of bone edema and its extension[11,12].

### *Chemical shift and DIXON*

Several types of advanced sequences have emerged as a technical optimization of chemical shift based on the DIXON technique. This technique acquires several TE at the same time and combines them to obtain, not only an "in phase" or "opposed phase" imaging, but also "fat only" and "water only" maps[13,14]. In this manner, time

**Table 1 Fat suppression techniques in musculoskeletal system**

| | In phase-out of phase | Fat saturation (CHESS) | Water excitation | DIXON | STIR | SPIR | SPAIR |
|---|---|---|---|---|---|---|---|
| Physical basis | Change of TE | Selective RF pulse that suppresses fat | Selective RF pulse that excites water | Different TEs, mathematic post-processing | Selective inversion of short T1 tissues | Spectrally selective RF pulse that suppresses fat | Spectrally adiabatic selective RF pulse that suppresses fat |
| Advantages | Fast<br>High SNR | High SNR<br>Contrast enhanced studies | Fast<br>3D acquisition | Four images in one acquisition<br>Quantification<br>Less prone to B0 and B1 | Less prone to B0 and B1 | Pre- and post-contrast studies | Insensitive to B1 |
| Drawbacks | Sensitivity to B0 | Sensitivity to B0 and B1 at large FOV | Sensitivity to B0 | Acquisition time | Suppress all short T1 structures | Sensitivity to B0 | Sensitivity to B0 |
| Clinical applications | Detection of bone infiltration | Bone edema evaluation in joints<br>MR-arthrography | Cartilage evaluation | All in one technique<br>High SNR<br>Less metal induced artifacts | Large FOV (spine)<br>Multiple interfaces (fingers, toes, metal) | Postcontrast imaging of inflammatory or neoplastic conditions | Large FOV and high SNR needed: thigh or MR-neurography |

CHESS: Chemical Shift Selective; STIR: Short inversion time recovery; SPIR: Spectral presaturation with inversion recovery; SPAIR: Spectral adiabatic inversion recovery; TE: Time of echo; RF: Radiofrequency; SNR: Signal noise ratio; FOV: Field of view.

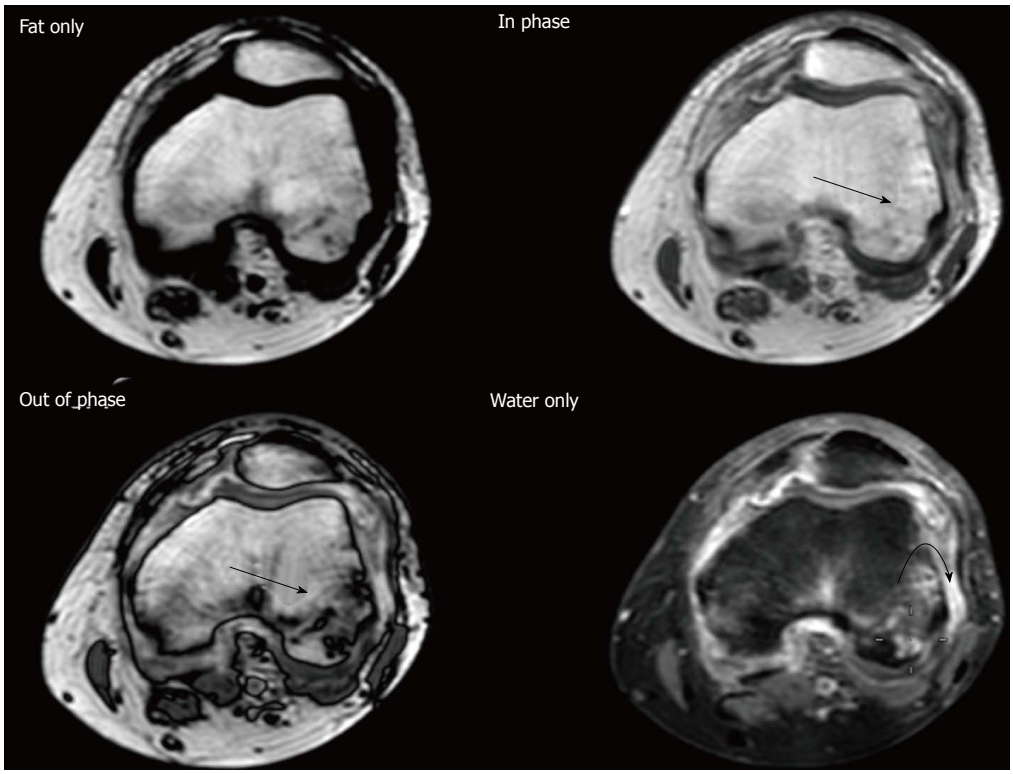


**Figure 1 DIXON.** Thirty-two years old woman with knee pain and suspected rheumatoid arthritis. Post-contrast DIXON study was performed. Opposed-phase image shows large hypointense areas in both condyles (arrows), which are hardly seen on the in-phase image, consistent with bone marrow edema. Note the presence of bone erosions and synovitis (curved arrow) better depicted on water only imaging.

can be saved by obtaining several stacks of images from only one acquisition (Figure 1).

The DIXON sequence is suitable for routine MRI to evaluate soft tissue and bone disorders and is compatible with a wide variety of pulse sequences, shcu as Turbo Spin Echo (TSE) and GE, and weightings (T2-weighted, T1-weighted or proton density images). The insensitivity of DIXON imaging to B0 and B1 heterogeneity offers robust fat suppression with higher SNR than other fat-suppressed techniques. Furthermore, the use of DIXON improves image quality in areas traditionally challenging for obtaining homogeneous fat-suppression, such as in regions of high magnetic susceptibility (*i.e.*, metallic implants) or in small anatomic areas, such as toes and fingers. DIXON sequences can be especially helpful in patients who cannot tolerate uncomfortable positions, particularly the pediatric and elderly populations[14,15], saving time in the acquisition of other sequences. Finally, DIXON provides quantitative parameters about water and fat

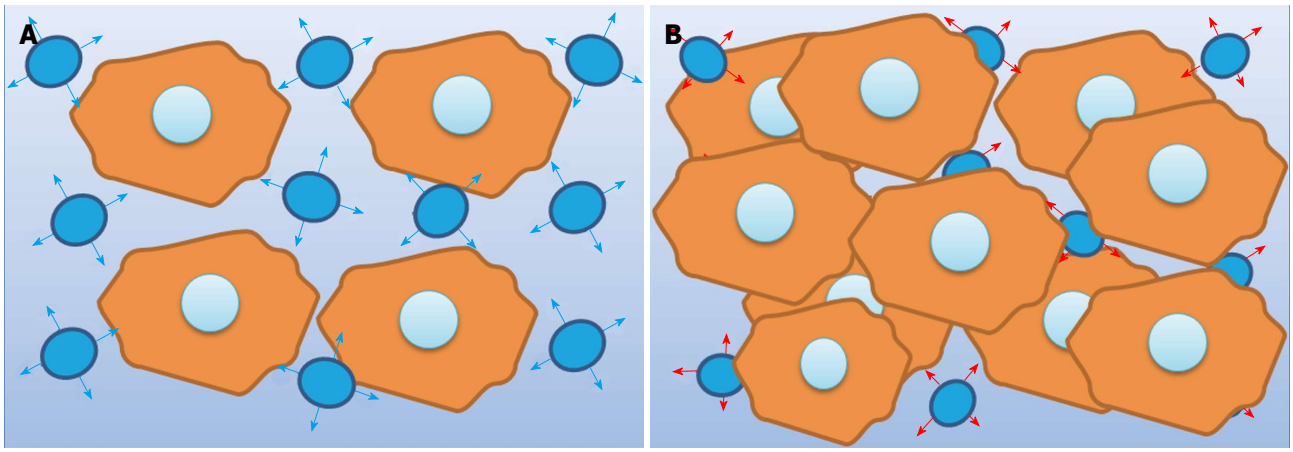


**Figure 2 Diffusion-weighted imaging.** A: Free water diffusion. The diagram represents the free motion of water molecules in the extracellular space between cells in normal tissue; B: Restricted water diffusion. The diagram represents the restricted motion of water molecules in the extracellular space due to hypercellularity. Another condition that leads to a decrease in the extracellular space is the presence of cytotoxic edema, while the presence of debris and detritus as in the case of abscesses may result also in restricted diffusion.

content of bone marrow and other tissues, including the percentage of signal loss between in phase and opposed phase images (fat fraction), which may provide potential biomarkers for treatment monitoring of arthritis[12,16]. Water only GE T1-weighted images provide high quality fat-suppression, which can be especially useful in dynamic postcontrast series or high-resolution late post-contrast studies, thereby improving the detection of subtle areas of enhancement[17].

### *DWI*

DWI evaluates the movement of free water within biological tissues. This property indirectly estimates cellularity and cell membrane integrity and allows for discrimination between hypercellular lesions and normal tissues[18] (Figure 2). DWI provides quantitative information through the Apparent Diffusion Coefficient (ADC) that represents the exponential decay of a single component of diffusion signal. DWI improves detection of malignant lesions which show reduced water motion secondary to the occupancy of the interstitial space by malignant cells. Furthermore, it has been proposed as an important oncological biomarker due to its ability to discriminate between malignant and benign lesions[19]. In a similar fashion, infection and inflammation demonstrate reduced water motion and restriction of diffusion. In this manner, DWI and ADC have demonstrated its ability for lesion characterization and treatment monitoring in musculoskeletal applications[20].

Specific technical adjustments are necessary to perform DWI in musculoskeletal radiology. Most commonly, DWI is performed using a single shot-echo planar imaging (SS EPI) sequence, which is prone to susceptibility and motion artifacts, that are usual in joint evaluation, especially in fingers and toes, due to air-bone-soft tissue interfaces. For bone evaluation, as well as for other anatomical regions, multi-channel or surface coils are usually needed for parallel imaging in order to obtain adequate SNR and reduce artifacts[21].

DWI provides a qualitative and quantitative assessment of arthritis in a relative short scan time and without need for exogenous contrast[22]. Normal bone marrow demonstrates low signal intensity on DWI images with low ADC values due to its low cellularity and scarce free water content and dominance of fatty tissue, especially in yellow (fatty) marrow. Characteristically, active arthritis will appear as areas of high signal on highly-weighted diffusion images, also known as high b values images, with concomitant decreased signal on ADC maps. As mentioned previously, one benefit of DWI is that the use of contrast agents is not required. This is particularly important for patients with joint diseases, as it is not uncommon for these patients to have an underlying systemic disease with renal function impairment. In this population, the administration of gadolinium chelates should be taken with caution to decrease the potential risk of develop nephrogenic systemic fibrosis. Also, children with juvenile idiopathic arthritis have inherent drawbacks for intravenous puncture[23]. In this setting, DWI can be considered as an alternative to contrast-enhanced sequences.

For articular disease assessment, DWI may also be used for soft tissue evaluation, particularly for synovial involvement, joint effusion characterization, and bone marrow edema detection thanks to its ability to assess the water molecules movement.

### *DCE MRI*

Conventional delayed postcontrast T1-weighted sequences only provide morphological information about areas of enhancement. DCE-MRI goes beyond conventional postcontrast MRI by providing pathophysiological information of the inflammatory processes themselves. DCE-MRI is usually based on a 3D gradient echo sequence with high temporal resolution, applying a dynamic scan faster than 4 s per dynamic[24]. This approach with high temporal resolution has shown several advantages over conventional multi-phase DCE-MRI (temporal resolution

**Table 2 Main parameters derived from dynamic contrast enhanced-magnetic resonance imaging studies**

| Parameter | Biological meaning |
|---|---|
| Area under the curve | The integral in a plot of concentration of contrast agent in blood plasma against time |
| Maximum (relative) enhancement | The maximum signal difference between the signal intensity at its maximum and baseline |
| Time to peak | Time elapsed between the arterial peak and the end of the steepest portion of enhancement |
| Wash in rate | The maximum slope between the time of onset of contrast inflow and the time of peak enhancement on the time intensity curve |
| Wash out rate | The clearance rate of contrast agent |
| $K^{trans}$ | Volume transfer constant between blood plasma and EES |
| $K^{ep}$ | Rate constant between EES and blood plasma |
| Ve | Volume of EES per unit of volume of tissue |

EES: Extravascular extracellular space.

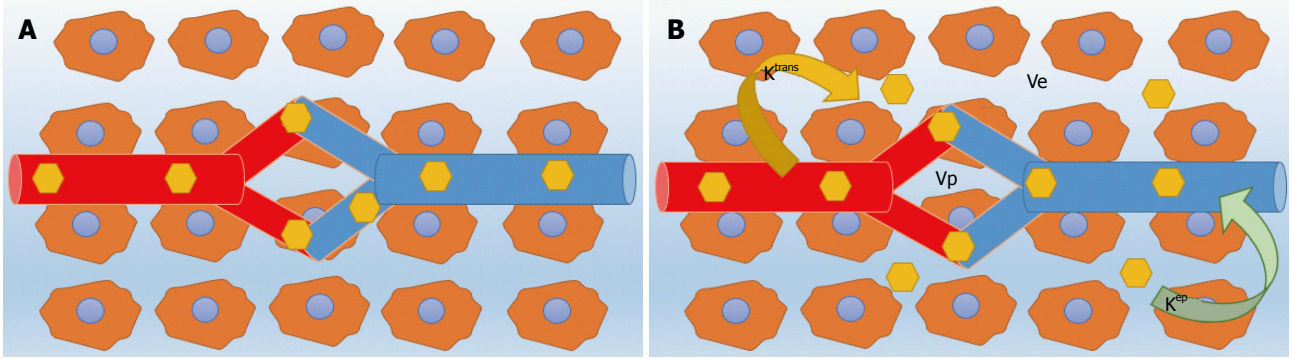


**Figure 3 Dynamic-contrast enhanced-magnetic resonance imaging.** Dynamic-contrast enhanced-magnetic resonance imaging analysis may be performed using a monocompartmental or a bicompartmental model. A: Diagram represents a monocompartmental model in which only vascular space is considered for distribution of gadolinium chelate; B: Diagram represents a bicompartmental model in which, besides the vascular space, the extracellular extravascular space with leakage and recirculation of gadolinium molecules are also considered. The main parameters derived for those models are detailed in Table 2.

between 12 to 20 s) with improved assessment of the dynamic enhancement process (Figure 3). New 4D acquisitions that combine high temporal and spatial resolution are able to provide simultaneous assessment of both structural and vascular properties[25]. This technique also permits MR-angiography reconstructions of regional vasculature.

In joint disease, the target structure on DCE-MRI is the synovium. DCE-MRI helps to understand the specific and complex physiopathological process that underlies each specific type of arthritis. The differential diagnosis may be narrowed based on the enhancement characteristics of the synovium, along with bone edema pattern and its distribution. The most helpful features for distinguishing the etiology of the joint process is the steepness and speed of enhancement during the first phases of DCE-MRI. For example, significant differences have been found in relative enhancement rate (RER), not in the first phases, but at delayed acquisition 15 min after Gad injection, with greater RER in rheumatoid arthritis (RA) than in psoriatic arthritis (PA). These results are a reflection of histopathology of synovitis in RA which presents higher cellularity and greater number of vessels compared with PA[26].

The analysis of DCE-MRI images has been classically performed using regions of interest (ROI). ROI-based analysis provides an average of all data included on a usually freehand drawn area[27,28]. Although widely used, this method is prone to sample errors. Other semi-automatic analysis methods have been proposed, using pixel by pixel maps of signal intensity data recorded on DCE-MRI studies[28,29].

Several types of time-intensity curves (TIC) have been described depending on the morphology and shape of the enhancement curve[30,31]. Type Ⅰ TIC is no enhancement, type Ⅱ curve reflects a slowly and progressively rising enhancement. Type Ⅲ TIC has a fast wash-in phase followed by a plateau and Type Ⅳ curve demonstrates fast wash-in and an early wash-out phase, usually linked to inflammatory activity. Finally, type Ⅴ is related to a fast wash-in with later progressive enhancement[27,32].

Parameters derived from monocompartmental or bicompartmental models of analysis of DCE studies are being considered as potential biomarkers for arthritis evaluation[33]. These biomarkers may predict aggressiveness of the arthritis and potentially aid in treatment monitoring[34]. Table 2 summarizes the main parameters derived from DCE-MRI studies and its biological meaning.

### *Cartilage imaging*

Imaging of cartilage is one of the primary goals for MRI of the joints. The loose of the normal physiologic

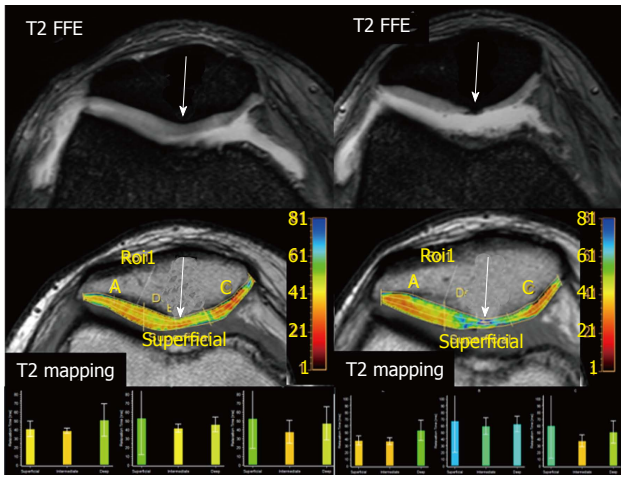


**Figure 4 Osteoarthritis progression.** A 49-year-old woman with knee pain is studied with two consecutive MRI studies. The first MRI (left images) shows a moderate joint effusion with patchy areas of increased signal intensity on T2 FFE sequence within the patellar cartilage. T2 mapping demonstrates diffuse increase in T2 relaxation times, more conspicuous at the patellar apex (arrows) consistent with early cartilage damage. Follow-up MRI performed 15 mo later (right images), demonstrates severe cartilage thinning, especially at patellar apex, that correlates with a severe increase in T2 relaxation times on the T2 mapping study. This clinical example demonstrates how T2 mapping can help to detect patients with evidence of early OA. MRI: Magnetic resonance imaging; OA: Osteoarthritis.

extracellular matrix precedes the development of bone damage and joint deformity. Articular hyaline cartilage has been classically evaluated with MRI using a morphological approach, which is limited due to the absence of pathophysiological information. In the last two decades, several functional sequences have been developed to allow a better understanding of cartilage structure. Functional MRI provides a qualitative and quantitative leap in early cartilage damage detection and treatment monitoring.

Nowadays, the most commonly applied functional technique for assessment of cartilage damage is T2 mapping. To obtain these images, multiple TE are acquired within the same sequence, computing the T2 relaxation time for each of those acquisitions. A voxel-based parametric map is generated showing the T2 relaxation time of cartilage, which can be assessed visually (qualitative analysis) or quantitative (ROI-based analysis)[35]. T2 relaxation time depends on the amount of water and the integrity of extracellular matrix, mainly secondary to collagen fiber density. The chemical interaction of collagen fibers with water protons results in a shortening of T2 relaxation time of the normal cartilage (Figure 4). There is a direct correlation between T2 values and water content and an inverse correlation with collagen concentration[36]. In this manner, areas of injured cartilage show a decrease in extracellular matrix (mainly collagen and proteoglycans) and increased water content. By increasing the TE, T2 mapping can detect these areas of early injury.

## CLINICAL SCENARIOS

### *Infectious arthritis*

The most frequent cause of septic arthritis is direct invasion through a skin defect/ulcer or haematogenous spread. In other cases, the infection is related to previous joint replacement surgery. Clinical and biochemical criteria are usually enough for an appropriate diagnosis, however in many cases, imaging is needed in order to evaluate the extent of the infection, particularly to evaluate for bone involvement. MRI has demonstrated a high accuracy for septic arthritis assessment[37,38]. As will be discussed in the next section, the introduction of functional MRI sequences may improve the specificity of the diagnosis, especially in evaluating the physiologic characteristics of the synovium, joint fluid, and neighboring bone.

DWI has shown potential for assessing joints and synovial fluid. One of the most useful applications of DWI in joint assessment is the evaluation of joint fluid and periarticular collections, in particular for depiction of infectious synovitis. In inflammatory fluid, hyaluronidases disrupt hyaluronic chains (that confer fluid viscosity) resulting in an increase in ADC values[39] (Figure 5). On the other hand, in septic arthritis, the presence of inflammatory cells, detritus, and pus produces an increase in viscosity which results in lower ADC values[40] (Figure 6). Thus, DWI is able to determine the nature of synovial fluid without the need for contrast agent injection and may also obviate the need for arthrocentesis, reducing potential complications such as infection and haemorrhage.

DWI has also demonstrated high accuracy in the differentiation between synovial thickening and reactive joint effusion, with high signal intensity at synovium on high b values due to hypercellularity. In cases of synovial thickening, intermediate ADC values (1.3-2.2 × $10^{-3}$ $mm^2/s$) may be found due to increased vascularization and associated perfusion-related effects in the synovium[20,40].

In cases of reactive bone involvement, there will be an increase in signal intensity on high b value DWI with concomitant high ADC values compared with normal bone due to the increase in water content of the damaged subchondral bone. When subchondral bone is affected by septic arthritis (osteomyelitis), involved areas will show hyperintensity at high b values with low ADC values due to the presence of pus and inflammatory cells[41].

DCE-MRI is also able to discriminate between synovial thickening and effusion and allows for the assessment of soft tissue involvement, synovitis (Figure 7), and necrotic areas in severe septic arthritis[42].

Postcontrast fat suppressed T1-weighted sequences usually help in the detection of bone marrow involvement as areas of increased enhancement. Normal yellow marrow will show no significant change in signal intensity after contrast injection compared to baseline. Involved bone in joints with septic arthritis will show a characteristic TIC (type II curve), with an intense early enhancement and later slight progressive increase of the enhancement slope compared to baseline marrow, without evidence of delayed washout[43]. Perfusion of epiphysis of involved bone has been shown to be lower

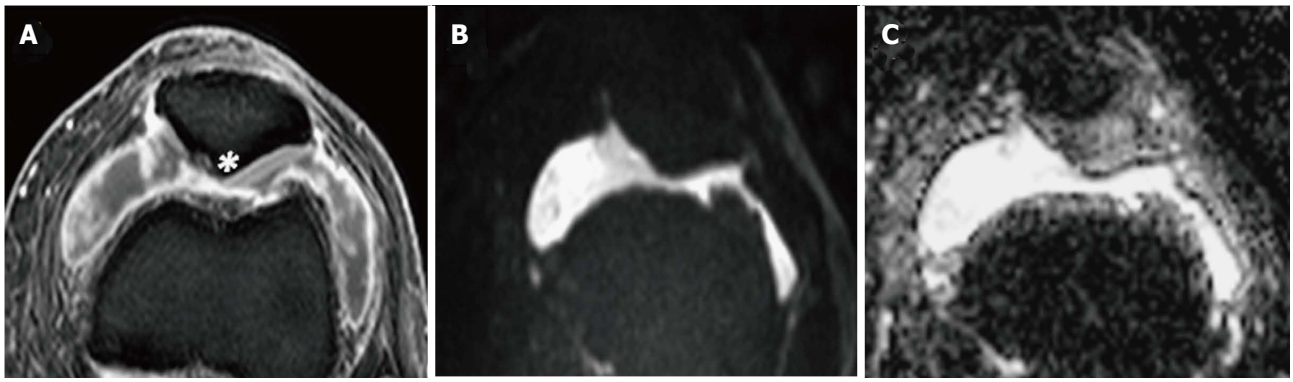


**Figure 5 Synovial fluid evaluation with diffusion-weighted imaging.** In a 42-year-old woman with RA and knee swelling. A: Axial post contrast fat-suppressed TSE T1-weighted sequence shows articular fluid and synovial enhancement; B, C: DWI with a b value of 900 s/mm$^2$ and corresponding ADC map confirm the presence of an effusion without significant restriction of free water motion (ADC: 2, 8 × 10$^{-3}$ mm$^2$/s) consistent with transudate due to rheumatoid arthritis, as confirmed by arthrocentesis. In this case, DWI helps to exclude infection. Note the presence of a prominent chondral erosion near to patellar apex (asterisk on A). DWI: Diffusion-weighted imaging; RA: Rheumatoid arthritis; ADC: Apparent diffusion coefficient.

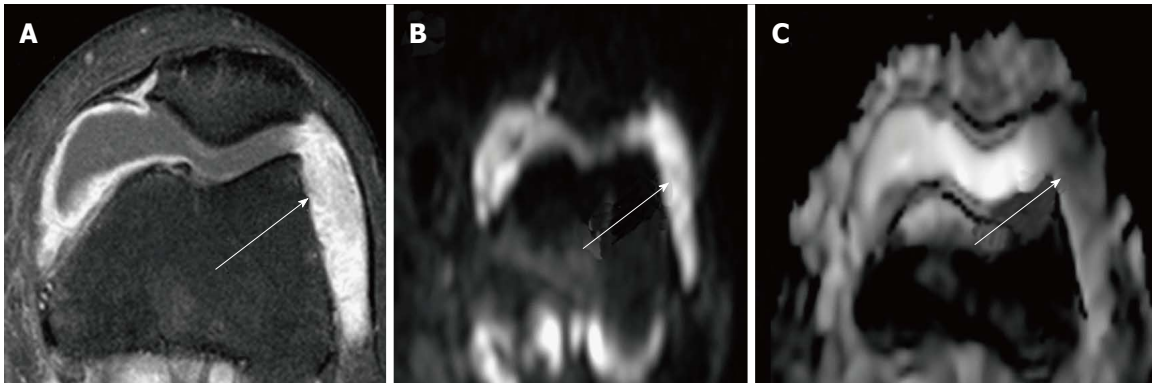


**Figure 6 Septic synovitis.** Magnetic resonance imaging findings in a 22-year-old man with knee pain and fever. A: Axial post contrast fat-suppressed TSE T1-weighted image shows a large joint effusion with synovial thickening and intense enhancement; B, C: DWI with a b value of 800 s/mm$^2$ and corresponding ADC map demonstrate areas of severely restricted diffusion (ADC: 1, 8 × 10$^{-3}$ mm$^2$/s) within the articular fluid at the lateral patellar recess consistent with exudate, as proven by arthrocentesis. DWI: Diffusion-weighted imaging; ADC: Apparent diffusion coefficient; TSE: Turbo spin echo.

than expected on the initial phases of DCE-MRI likely due to an increase in hydrostatic pressure or possibly septic thrombosis of epiphyseal vessels. Furthermore, these changes may lead to avascular necrosis[44].

### *Inflammatory arthritis*

**Sacroiliitis:** For sacroiliitis (SI) evaluation, conventional fat suppression techniques have high accuracy but a relative lack of specificity in the discrimination between early acute and sub-acute disease. Recently, several reports have focused on the potential of DWI to assess the sacroiliac joints, given its ability to detect subchondral bone edema with similar accuracy to fat suppressed contrast-enhanced T1-weighted images[45]. This may determine the degree of activity in acute sacroiliitis, although with lesser SNR than fat suppressed T2-weighted sequences[46]. In active sacroiliitis, areas of high signal intensity will be detected on high b value images in the subchondral bone but with higher ADC values than normal bone marrow, reflecting the presence of an inflammatory process. In chronic sacroiliitis, due to fatty changes, the involved joint will show lower signal intensity on high b value images and lower ADC values than normal bone marrow (Figure 8)[47].

DWI has also been shown to increase the conspicuity of bone subchondral edema, likely related to a proper suppression of background signal, and thus may increase the specificity of these changes in patients with early SI. Higher ADC values (0.5-1.5 × 10$^{-3}$ mm$^2$/s) have been found in affected subchondral bone compared with control groups (0.2-0.6 × 10$^{-3}$ mm$^2$/s)[48].

Post contrast fat suppression T1-weighted images as well as DCE-MRI have demonstrated its usefulness for SI detection with higher accuracy of the latter for detection of active disease even in the earliest phases[49].

**Rheumatoid arthritis:** Rheumatoid arthritis (RA) pathogenesis starts with an autoimmune inflammatory reaction against antigens located at the synovium that usually results in eventual joint destruction. As in SI, MRI has demonstrated to be superior to conventional imaging for detection of RA even in early phases[2].

Detection and characterization of synovitis and subchondral bone edema are the primary focus of MRI,

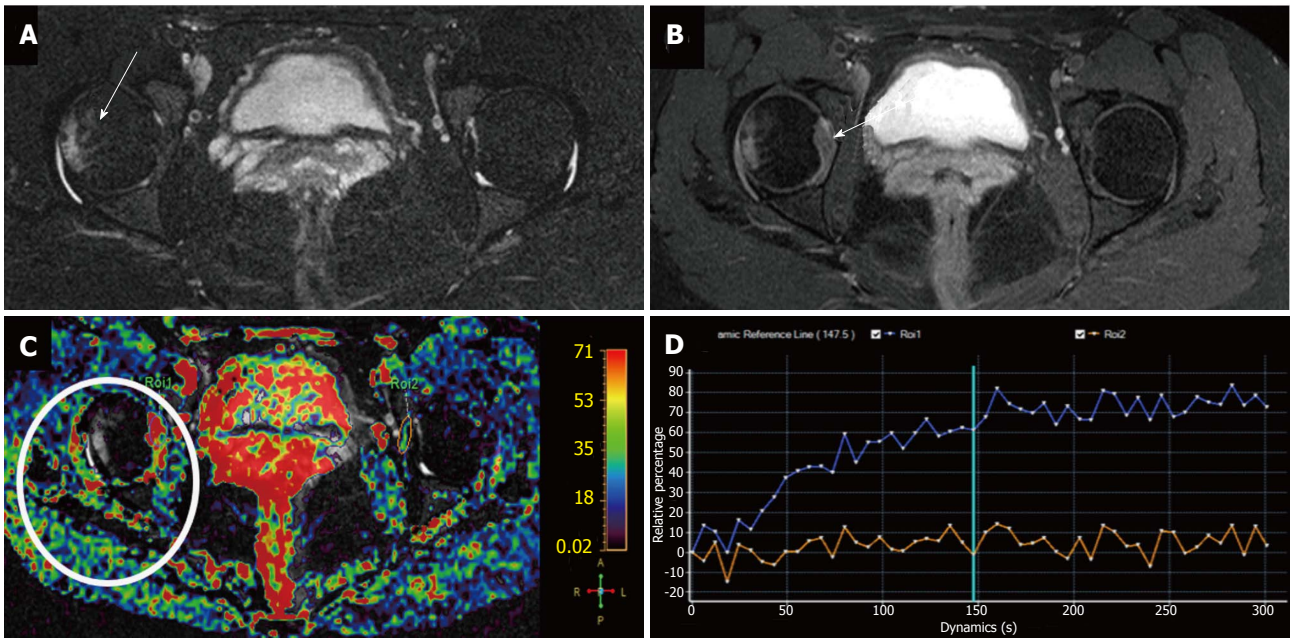


**Figure 7 Evaluation of inflammatory arthritis with dynamic-contrast enhanced-magnetic resonance imaging in a 42-year-old woman with rheumatoid arthritis and right hip pain**. A: Axial STIR shows mild articular effusion in the right hip with subtle signs of subchondral bone edema (arrow); B: Axial post-gadolinium SPIR GE T1-weighted image demonstrates moderate synovial thickening and enhancement especially at the medial articular surface (arrow); C: Relative enhancement map; D: Dynamic-contrast enhanced-magnetic resonance imaging demonstrate a type I TIC (blue curve) in the right hip, with progressive enhancement, compared to absence of significant enhancement in the contralateral hip (orange curve). This finding helps to confirm the inflammatory involvement of right hip. STIR: Short inversion time recovery.

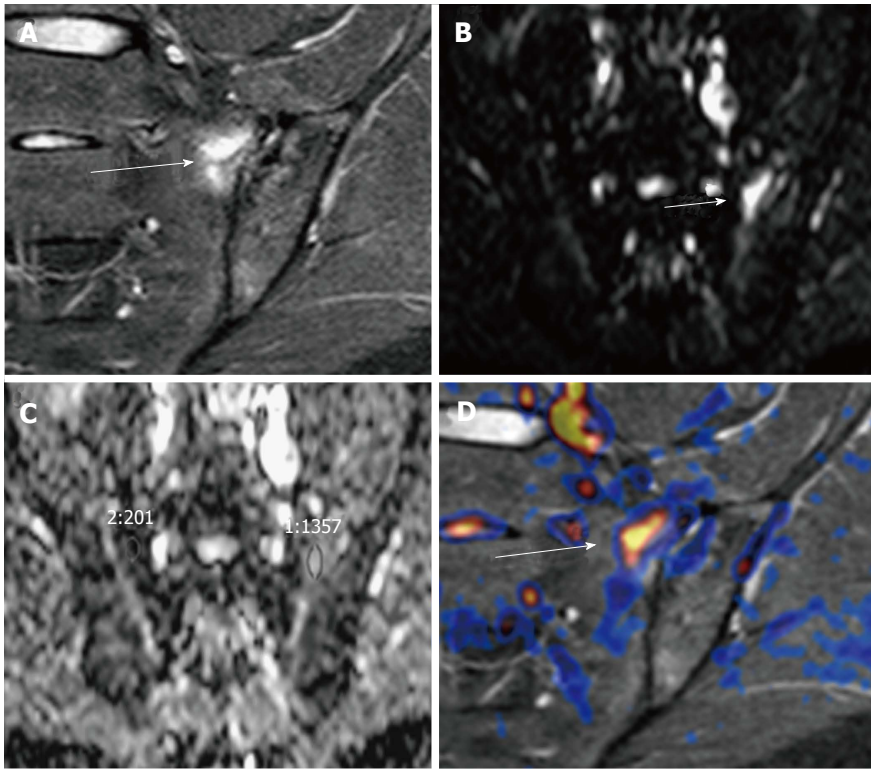


**Figure 8 Acute sacroiliitis in a 32-year-old woman with left hip pain**. A-C: Coronal STIR shows a focus of subchondral bone edema in the left hemisacrum (arrow, A), which appears hyperintense on (B) high *b* value DWI, with (C) significantly higher ADC values than contralateral bone marrow ($1.3 \times 10^{-3}$ $mm^2/s$ *vs* $0.2 \times 10^{-3}$ $mm^2/s$); D: Fused DWI and STIR images allow a better depiction of bone edema. STIR: Short inversion time recovery; DWI: Diffusion-weighted imaging; ADC: Apparent diffusion coefficient.

as these features have been demonstrated to be the strongest predictors of early RA and bone erosions, respectively[50]. These characteristics have been included in a MRI scoring system for RA evaluation (RAMRIS),

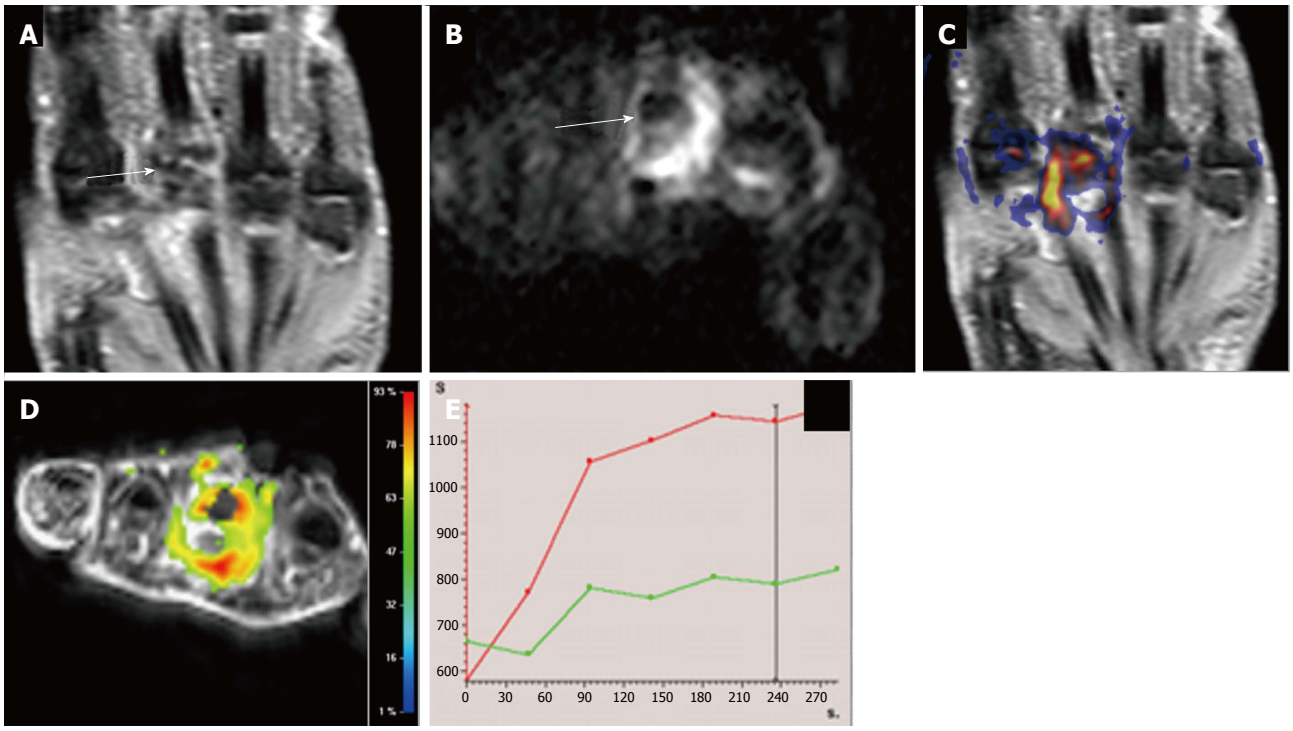


**Figure 9 Multiparametric evaluation of rheumatoid arthritis in a 40-year-old woman with hand involvement.** A: Coronal STIR shows severe articular surface erosions with subchondral edema and synovial hypertrophy at the 3rd metatarsal-phalangeal joint (arrow); B: Axial DWI b800 demonstrates markedly restricted diffusion within this joint (arrow, B) with good correlation on (C) STIR and DWI b 800 fused image; D, E: (D) DCE-MRI relative enhancement map shows increased enhancement and (E) TIC of the involved joint (red curve) shows an initial fast enhancement which becomes more progressive and slow in late phases in comparison to the adjacent normal joint (green curve). STIR: Short inversion time recovery; DWI: Diffusion-weighted imaging; MRI: Magnetic resonance imaging; DCE: Dynamic contrast enhancement.

as indicator of disease activity[51]. Fat suppression techniques have improved the ability of MRI for bone edema detection as discussed previously.

Functional sequences like DWI and DCE-MRI have also contributed to the increase in overall accuracy of MRI for RA assessment, providing several quantitative parameters which may be used as biomarkers of RA activity[2]. DWI has demonstrated a high accuracy for synovitis detection in the wrist and hand, especially in the metacarpophalangeal and proximal phalangeal joints, in patients with RA[52]. Synovial infiltration by inflammatory cells may affect the mobility of water molecules (Figure 9). Furthermore, the inherent background suppression of surrounding tissues increases the sensitivity and specificity of DWI over other MRI techniques for synovitis and bone edema detection, which have been linked to rapid radiographic progression in patients with early signs of RA[51,52]. One downside of DWI is the susceptibility to inhomogeneities in the magnetic field and low SNR, limiting its application in assessment of the hands and feet.

The interest of applying DCE-MRI studies for the evaluation of RA, particularly in the assessment of synovitis, is rising nowadays, as it has demonstrated a high correlation with clinical, biochemical, and histological markers of disease activity[33]. The steepness of the TIC in cases of active disease, usually demonstrating a fast initial enhancement phase and later plateau or washout, better reflects the physiopathological process behind synovitis than the single use of pre and post-gad T1 sequences. Semi-quantitative parameters such as maximum enhancement (ME) and rate of early enhancement (REE) may be used as potential biomarkers and allow the detection of changes in synovial vasculature before changes in synovial volume or bone edema occur[53].

Besides clinical and biochemical criteria, DCE-MRI has demonstrated the ability to discriminate between RA and psoriatic arthritis (PA), as previously discussed. A significant difference is in the relative enhancement rate (RER), at delayed acquisition 15 min after gadolinium injection has been reported between both entities. These results are a reflection of histopathology of synovitis in RA which has a higher cellularity and a greater number of recruited vessels compared with PA[26].

**Juvenile idiopathic arthritis:** Juvenile idiopathic arthritis has also been successfully evaluated with classical morphological MRI sequences, and more recently with functional imaging with promising results for the assessment of knee, wrist, and hip involvement[54,55]. DWI has several advantages in the depiction of bone edema and synovitis in young patients, including the lack of ionizing radiation, the ability to assess active and subclinical synovitis in patients with a difficult clinical examination, the identification of high-risk patients, and ultimately, in treatment monitoring[20].

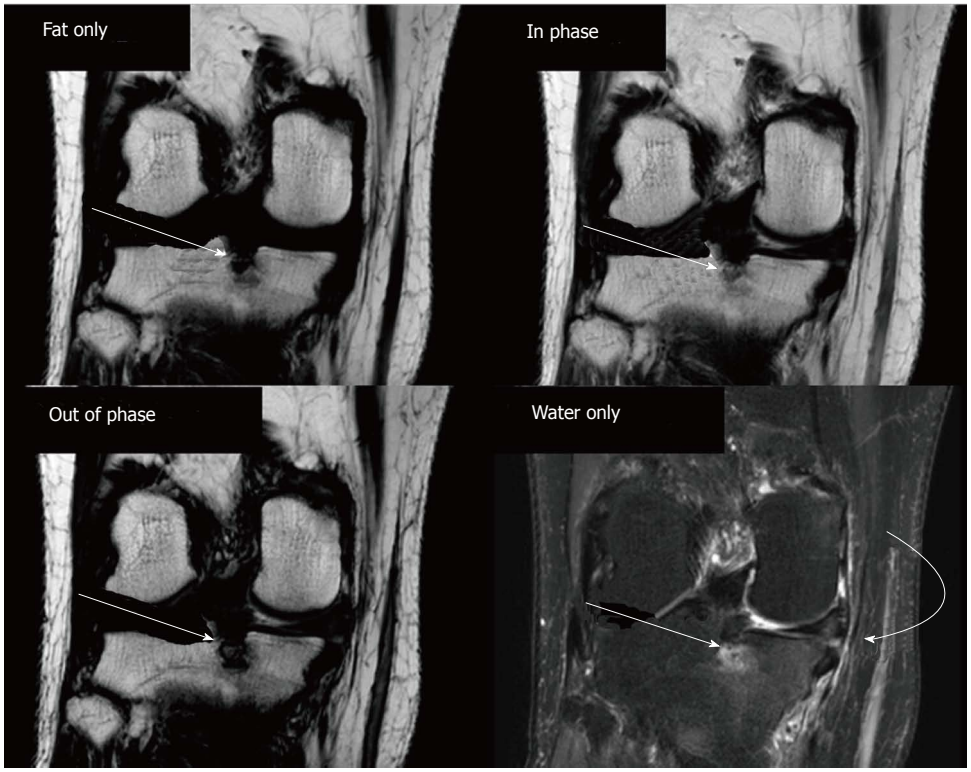


**Figure 10 DIXON for evaluation of osteoarthritis in a 56-year-old woman with chronic knee pain**. A subchondral geode is identified at the medial aspect of the medial tibial plateau (arrow), which is more conspicuous in the opposed-phase image than in the in-phase image suggesting edematous changes, as confirmed in the water-only acquisition. The water only image also shows soft tissue edema at the body of the medial meniscus and medial collateral ligament (curved arrow).

Finally, DCE-MRI has been proposed as a potential biomarker in children with juvenile idiopathic arthritis and wrist involvement demonstrating an association between clinical active disease and derived-parameters such as maximum relative enhancement[56].

### *Osteoarthritis*

The active erosive changes that occur in the first phases of osteoarthritis (OA) may be studied by functional MRI sequences. If treatment is introduced in this phase, before reparative changes occur, the course of the disease may be altered enough to avoid joint deformities.

Based on DCE-MRI, differences between RA and OA can be found that reflects the different physiopathology of RA (inflammatory) and OA (degenerative). OA shows higher semi-quantitative (REE) and quantitative ($K^{trans}$, $K^{ep}$) values than control subjects, but lower ones than those in RA, likely due to an inferior angiogenic potential and decreased permeability of synovium in OA[57].

Joint imaging requires multiple planes and several fat-suppression sequences, factors that prolong the total scan time. Some studies have demonstrated that CSI and DIXON techniques, through in-phase and out of phase sequences as well as through the use of water only images, can accurately assess subchondral bone thickness while reducing the scan time (Figure 10)[58].

Early detection of cartilage damage may allow the treatment of patients with potentially better outcomes than in advanced OA stages[59]. As previously discussed, T2 mapping techniques are able to detect areas of elevated T2 values within normal-appearing hyaline cartilage on morphological sequences[60,61]. In OA, cartilage damage is usually present at high pressure points, unlike in RA and other inflammatory arthritis whereas can be seen at any area of cartilage joint surface[62].

### *Therapy monitoring*

Functional MRI techniques for joint evaluation can be also used in treatment monitoring. As drugs used for modulation of articular disease progression in SI and other inflammatory arthritis have non-negligible adverse side effects, these advanced MRI sequences may accurately determine the effectiveness of treatment. Normalization of ADC values and signal intensity on DWI is related to proper treatment response, while the presence of high ADC values after treatment may reflect persistence of inflammatory signs[63]. For example, for SI, DWI has demonstrated the potential to be a tool for therapy monitoring of active sacroiliitis[47,63,64]. In inflammatory arthritis, the response to steroid and non-steroid anti-inflammatory drugs can be assessed by reduction of angiogenesis in DCE- derived parameters[65]. In a similar manner, in septic arthritis, DCE-MRI can aid in the assessment of response to antibiotherapy (Figure 11). Parameters derived from pharmacokinetic models, such as $K^{trans}$ and $K^{ep}$, are also elevated in patients with RA, reflecting the increase in perfusion, extravascular space, and permeability in synovitis. Their reduction after successful treatment provides a mechanism for noninvasive

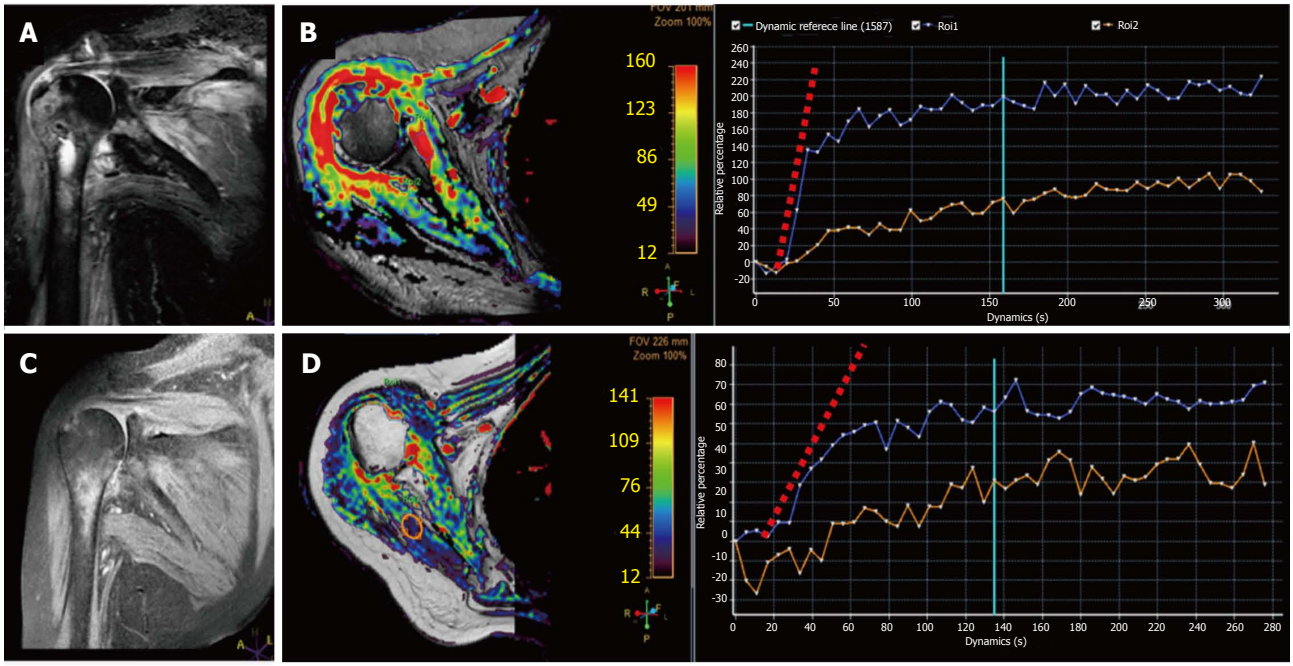


**Figure 11 Magnetic resonance follow-up of septic arthritis in a 58-year-old woman with shoulder pain, fever, and swelling**. A: Coronal STIR shows severe edema within the proximal humerus as well as in the surrounding soft tissues with minimal intraarticular fluid; B: DCE-MRI relative enhancement map demonstrates extensive enhancement in the synovium and the humeral head; C, D: Follow-up MRI study 3 wk after intravenous antibiotic therapy demonstrates adequate response to treatment with reduction of edema on STIR and enhancement on DCE-MRI. Note also the change in the initial slope of the blue TIC (synovial enhancement) between pre and post-treatment studies. The orange TIC shows healthy muscle contrast enhancement as an internal reference. STIR: Short inversion time recovery; DWI: Diffusion-weighted imaging; MRI: Magnetic resonance imaging; DCE: Dynamic contrast enhancement.

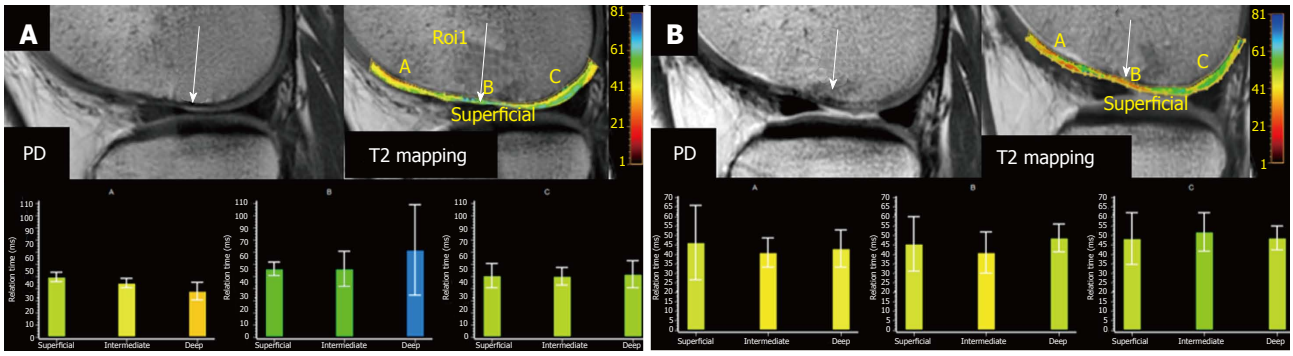


**Figure 12 Treatment monitoring with magnetic resonance imaging in a 26-year-old gymnast with knee pain.** Initial MRI (A) shows mild cartilage thinning at the medial femoral condyle with subchondral damage PD image. A moderate increase in T2 relaxation values (arrow) confirms the loss of collagen fibers in this area. Patient underwent MTX therapy and a follow-up MRI performed 3 mo later (B) demonstrates moderate chondral irregularity with focal areas of increased signal intensity on PD. T2 mapping demonstrates normalization of T2 relaxation time values compared with the pre-treatment study due to the generation of new fibrous cartilage. MRI: Magnetic resonance imaging; MTX: Microfracturing therapy; PD: Proton-density images.

treatment monitoring[31]. These parameters also allow for the discrimination between patients with active disease from inactive disease and healthy persons[66].

In a similar manner, for OA treatment monitoring, new specific drugs and cartilage repairing techniques have been developed trying to slow, or even revert, the progression of OA. Thus, accurate imaging biomarkers that can provide an earlier diagnosis of OA and can detect immediate signs of progression during treatment monitoring are crucial. The effectiveness of these treatments is closely related to their early introduction at the first stages of OA. Surgical techniques in patient with chondromalacia such as microfracturing therapy (MTX) and matrix autologous chondrocyte transplantation (MACT) are now used in clinical practice, and functional MR sequences may be able to assess the success or failure of the surgical intervention[67]. T2 values of the repaired tissue after MTX is initially lower than after MACT due to the presence of repairing fibrous cartilage rather than hyaline cartilage (Figure 12). However, during long-term follow-up, T2 values of the repaired cartilage in patients treated with MTX tend to normalize in comparison to the rest of cartilage. If this normalization does not occur, a therapy failure may

be considered[68].

## CONCLUSION

The introduction of MRI for joint evaluation has improved the assessment of arthropathies. However, in many cases, conventional MRI studies are insufficient for a specific diagnosis and limited in their assessment of treatment success. A wide range of advanced MRI techniques are now available in musculoskeletal radiology and can be applied for evaluating arthritis. Technical improvements in fat suppression sequences such as DIXON enable a faster and better detection of bone involvement. DWI and DCE-MRI provide pathophysiological information regarding the cellularity and vascularization of bone and soft tissue in joint diseases, which can aid in determining the specific type of arthritis, the extent of disease, and the success or failure of treatment. T2 mapping allows the evaluation of early cartilage damage before conventional sequences, leading to earlier, and thus potentially more successful, treatment. Integration of these functional techniques within conventional protocols should be considered not only for diagnostic purposes but also for treatment monitoring of arthropathies.

## REFERENCES


1 **Kim JY**, Choi YY, Kim CW, Sung YK, Yoo DH. Bone Scintigraphy in the Diagnosis of Rheumatoid Arthritis: Is There Additional Value of Bone Scintigraphy with Blood Pool Phase over Conventional Bone Scintigraphy? *J Korean Med Sci* 2016; **31**: 502-509 [PMID: 27051232 DOI: 10.3346/jkms.2016.31.4.502]

2 **Krabbe S**, Bolce R, Brahe CH, Døhn UM, Ejbjerg BJ, Hetland ML, Sasso EH, Chernoff D, Hansen MS, Knudsen LS, Hansen A, Madsen OR, Hasselquist M, Møller J, Østergaard M. Investigation of a multi-biomarker disease activity score in rheumatoid arthritis by comparison with magnetic resonance imaging, computed tomography, ultrasonography, and radiography parameters of inflammation and damage. *Scand J Rheumatol* 2016; Epub ahead of print [PMID: 27682742 DOI: 10.1080/03009742.2016.1211315]

3 **Chen J**, Liao M, Zhang H, Zhu D. Diagnostic accuracy of dual-energy CT and ultrasound in gouty arthritis : A systematic review. *Z Rheumatol* 2017; Epub ahead of print [PMID: 28058498 DOI: 10.1007/s00393-016-0250-8]

4 **Möller I**, Loza E, Uson J, Acebes C, Andreu JL, Batlle E, Bueno Á, Collado P, Fernández-Gallardo JM, González C, Jiménez Palop M, Lisbona MP, Macarrón P, Maymó J, Narváez JA, Navarro-Compán V, Sanz J, Rosario MP, Vicente E, Naredo E. Recommendations for the use of ultrasound and magnetic resonance in patients with rheumatoid arthritis. *Reumatol Clin* 2016; Epub ahead of print [PMID: 28029551 DOI: 10.1016/j.reuma.2016.08.010]

5 **Vyas S**, Bhalla AS, Ranjan P, Kumar S, Kumar U, Gupta AK. Rheumatoid Arthritis Revisited - Advanced Imaging Review. *Pol J Radiol* 2016; **81**: 629-635 [PMID: 28105245 DOI: 10.12659/PJR.899317]

6 **Lee S**, Lee JY, Hwang JH, Shin JH, Kim TH, Kim SK. Clinical importance of inflammatory facet joints of the spine in ankylosing spondylitis: a magnetic resonance imaging study. *Scand J Rheumatol* 2016; **45**: 491-498 [PMID: 27098409 DOI: 10.3109/03009742.2016.1150506]

7 **Narváez JA**, Narváez J, De Lama E, De Albert M. MR imaging of early rheumatoid arthritis. *Radiographics* 2010; **30**: 143-163; discussion 163-165 [PMID: 20083591 DOI: 10.1148/rg.301095089]

8 **Yang H**, Rivoire J, Hoppe M, Srikhum W, Imboden J, Link TM, Li X. Computer-aided and manual quantifications of MRI synovitis, bone marrow edema-like lesions, erosion and cartilage loss in rheumatoid arthritis of the wrist. *Skeletal Radiol* 2015; **44**: 539-547 [PMID: 25488101 DOI: 10.1007/s00256-014-2059-3]

9 **Delfaut EM**, Beltran J, Johnson G, Rousseau J, Marchandise X, Cotten A. Fat suppression in MR imaging: techniques and pitfalls. *Radiographics* 2014; **19**: 373-382 [PMID: 10194785 DOI: 10.1148/radiographics.19.2.g99mr03373]

10 **Del Grande F**, Santini F, Herzka DA, Aro MR, Dean CW, Gold GE, Carrino JA. Fat-suppression techniques for 3-T MR imaging of the musculoskeletal system. *Radiographics* 2014; **34**: 217-233 [PMID: 24428292 DOI: 10.1148/rg.341135130]

11 **Maas M**, Dijkstra PF, Akkerman EM. Uniform fat suppression in hands and feet through the use of two-point Dixon chemical shift MR imaging. *Radiology* 1999; **210**: 189-193 [PMID: 9885606 DOI: 10.1148/radiology.210.1.r99ja35189]

12 **Dreizin D**, Ahlawat S, Del Grande F, Fayad LM. Gradient-echo in-phase and opposed-phase chemical shift imaging: role in evaluating bone marrow. *Clin Radiol* 2014; **69**: 648-657 [PMID: 24613580 DOI: 10.1016/j.crad.2014.01.027]

13 **Douis H**, Davies AM, Jeys L, Sian P. Chemical shift MRI can aid in the diagnosis of indeterminate skeletal lesions of the spine. *Eur Radiol* 2016; **26**: 932-940 [PMID: 26162578 DOI: 10.1007/s00330-015-3898-6]

14 **Ma J**. Dixon techniques for water and fat imaging. *J Magn Reson Imaging* 2008; **28**: 543-558 [PMID: 18777528 DOI: 10.1002/jmri.21492]

15 **Kim HK**, Lindquist DM, Serai SD, Mariappan YK, Wang LL, Merrow AC, McGee KP, Ehman RL, Laor T. Magnetic resonance imaging of pediatric muscular disorders: recent advances and clinical applications. *Radiol Clin North Am* 2013; **51**: 721-742 [PMID: 23830795 DOI: 10.1016/j.rcl.2013.03.002]

16 **Moal B**, Bronsard N, Raya JG, Vital JM, Schwab F, Skalli W, Lafage V. Volume and fat infiltration of spino-pelvic musculature in adults with spinal deformity. *World J Orthop* 2015; **6**: 727-737 [PMID: 26495250 DOI: 10.5312/wjo.v6.i9.727]

17 **Park HJ**, Lee SY, Rho MH, Chung EC, Ahn JH, Park JH, Lee IS. Usefulness of the fast spin-echo three-point Dixon (mDixon) image of the knee joint on 3.0-T MRI: comparison with conventional fast spin-echo T2 weighted image. *Br J Radiol* 2016; **89**: 20151074 [PMID: 27008281 DOI: 10.1259/bjr.20151074]

18 **Costa FM**, Ferreira EC, Vianna EM. Diffusion-weighted magnetic resonance imaging for the evaluation of musculoskeletal tumors. *Magn Reson Imaging Clin N Am* 2011; **19**: 159-180 [PMID: 21129640 DOI: 10.1016/j.mric.2010.10.007]

19 **Padhani AR**, Liu G, Koh DM, Chenevert TL, Thoeny HC, Takahara T, Dzik-Jurasz A, Ross BD, Van Cauteren M, Collins D, Hammoud DA, Rustin GJ, Taouli B, Choyke PL. Diffusion-weighted magnetic resonance imaging as a cancer biomarker: consensus and recommendations. *Neoplasia* 2009; **11**: 102-125 [PMID: 19186405]

20 **Neubauer H**, Evangelista L, Morbach H, Girschick H, Prelog M, Köstler H, Hahn D, Beer M. Diffusion-weighted MRI of bone marrow oedema, soft tissue oedema and synovitis in paediatric patients: feasibility and initial experience. *Pediatr Rheumatol Online J* 2012; **10**: 20 [PMID: 22849717 DOI: 10.1186/1546-0096-10-20]

21 **Macarini L**, Stoppino LP, Milillo P, Ciuffreda P, Fortunato F, Vinci R. Diffusion-weighted MRI with parallel imaging technique: apparent diffusion coefficient determination in normal kidneys and in nonmalignant renal diseases. *Clin Imaging* 2010; **34**: 432-440 [PMID: 21092872 DOI: 10.1016/j.clinimag.2009.09.007]

22 **Khoo MM**, Tyler PA, Saifuddin A, Padhani AR. Diffusion-weighted imaging (DWI) in musculoskeletal MRI: a critical review. *Skeletal Radiol* 2011; **40**: 665-681 [PMID: 21311884 DOI: 10.1007/s00256-011-1106-6]

23 **Khawaja AZ**, Cassidy DB, Al Shakarchi J, McGrogan DG, Inston NG, Jones RG. Revisiting the risks of MRI with Gadolinium based contrast agents-review of literature and guidelines. *Insights Imaging* 2015; **6**: 553-558 [PMID: 26253982 DOI: 10.1007/s13244-015-0420-2]

24 **Maijer KI**, van der Leij C, de Hair MJ, Tas SW, Maas M, Gerlag DM,

Tak PP, Lavini C. Dynamic Contrast-Enhanced Magnetic Resonance Imaging Using Pharmacokinetic Modeling: Initial Experience in Patients With Early Arthritis. *Arthritis Rheumatol* 2016; **68**: 587-596 [PMID: 26473331 DOI: 10.1002/art.39469]

25 **Hadizadeh DR**, Marx C, Gieseke J, Schild HH, Willinek WA. High temporal and high spatial resolution MR angiography (4D-MRA). *Rofo* 2014; **186**: 847-859 [PMID: 24955647 DOI: 10.1055/s-0034-1366661]

26 **Schwenzer NF**, Kötter I, Henes JC, Schraml C, Fritz J, Claussen CD, Horger M. The role of dynamic contrast-enhanced MRI in the differential diagnosis of psoriatic and rheumatoid arthritis. *AJR Am J Roentgenol* 2010; **194**: 715-720 [PMID: 20173150 DOI: 10.2214/AJR.09.2671]

27 **van der Leij C**, van de Sande MG, Lavini C, Tak PP, Maas M. Rheumatoid synovial inflammation: pixel-by-pixel dynamic contrast-enhanced MR imaging time-intensity curve shape analysis--a feasibility study. *Radiology* 2009; **253**: 234-240 [PMID: 19703863 DOI: 10.1148/radiol.2531081722]

28 **Lavini C**, Pikaart BP, de Jonge MC, Schaap GR, Maas M. Region of interest and pixel-by-pixel analysis of dynamic contrast enhanced magnetic resonance imaging parameters and time-intensity curve shapes: a comparison in chondroid tumors. *Magn Reson Imaging* 2009; **27**: 62-68 [PMID: 18619754 DOI: 10.1016/j.mri.2008.05.012]

29 **Liu J**, Pedoia V, Heilmeier U, Ku E, Su F, Khanna S, Imboden J, Graf J, Link T, Li X. High-temporospatial-resolution dynamic contrast-enhanced (DCE) wrist MRI with variable-density pseudo-random circular Cartesian undersampling (CIRCUS) acquisition: evaluation of perfusion in rheumatoid arthritis patients. *NMR Biomed* 2016; **29**: 15-23 [PMID: 26608949 DOI: 10.1002/nbm.3443]

30 **Tokuda O**, Hayashi N, Taguchi K, Matsunaga N. Dynamic contrast-enhanced perfusion MR imaging of diseased vertebrae: analysis of three parameters and the distribution of the time-intensity curve patterns. *Skeletal Radiol* 2005; **34**: 632-638 [PMID: 16091963 DOI: 10.1007/s00256-005-0949-0]

31 **Lavini C**, Buiter MS, Maas M. Use of dynamic contrast enhanced time intensity curve shape analysis in MRI: Theory and practice. *Reports Med Imaging* 2013; **6**: 71-82

32 **Griffith JF**. Functional imaging of the musculoskeletal system. *Quant Imaging Med Surg* 2015; **5**: 323-331 [PMID: 26029633 DOI: 10.3978/j.issn.2223-4292.2015.03.07]

33 **van de Sande MG**, van der Leij C, Lavini C, Wijbrandts CA, Maas M, Tak PP. Characteristics of synovial inflammation in early arthritis analysed by pixel-by-pixel time-intensity curve shape analysis. *Rheumatology* (Oxford) 2012; **51**: 1240-1245 [PMID: 22375037 DOI: 10.1093/rheumatology/kes011]

34 **Conaghan PG**, Østergaard M, Bowes MA, Wu C, Fuerst T, van der Heijde D, Irazoque-Palazuelos F, Soto-Raices O, Hrycaj P, Xie Z, Zhang R, Wyman BT, Bradley JD, Soma K, Wilkinson B. Comparing the effects of tofacitinib, methotrexate and the combination, on bone marrow oedema, synovitis and bone erosion in methotrexate-naive, early active rheumatoid arthritis: results of an exploratory randomised MRI study incorporating semiquantitative and quantitative techniques. *Ann Rheum Dis* 2016; **75**: 1024-1033 [PMID: 27002108 DOI: 10.1136/annrheumdis-2015-208267]

35 **Mosher TJ**, Liu Y, Torok CM. Functional cartilage MRI T2 mapping: evaluating the effect of age and training on knee cartilage response to running. *Osteoarthritis Cartilage* 2010; **18**: 358-364 [PMID: 19948266 DOI: 10.1016/j.joca.2009.11.011]

36 **Kretzschmar M**, Bieri O, Miska M, Wiewiorski M, Hainc N, Valderrabano V, Studler U. Characterization of the collagen component of cartilage repair tissue of the talus with quantitative MRI: comparison of T2 relaxation time measurements with a diffusion-weighted double-echo steady-state sequence (dwDESS). *Eur Radiol* 2015; **25**: 980-986 [PMID: 25407662 DOI: 10.1007/s00330-014-3490-5]

37 **Karchevsky M**, Schweitzer ME, Morrison WB, Parellada JA. MRI findings of septic arthritis and associated osteomyelitis in adults. *AJR Am J Roentgenol* 2004; **182**: 119-122 [PMID: 14684523 DOI: 10.2214/ajr.182.1.1820119]

38 **Graif M**, Schweitzer ME, Deely D, Matteucci T. The septic versus nonseptic inflamed joint: MRI characteristics. *Skeletal Radiol* 1999; **28**: 616-620 [PMID: 10591923]

39 **Eustace S**, DiMasi M, Adams J, Ward R, Caruthers S, McAlindon T. In vitro and in vivo spin echo diffusion imaging characteristics of synovial fluid: potential non-invasive differentiation of inflammatory and degenerative arthritis. *Skeletal Radiol* 2000; **29**: 320-323 [PMID: 10929413]

40 **Park JK**, Kim BS, Choi G, Kim SH, Lee KB, Khang H. Distinction of reactive joint fluid from pyogenic abscess by diffusion-weighted imaging. *J Magn Reson Imaging* 2007; **25**: 859-861 [PMID: 17345641 DOI: 10.1002/jmri.20886]

41 **Subhawong TK**, Jacobs MA, Fayad LM. Diffusion-weighted MR imaging for characterizing musculoskeletal lesions. *Radiographics* 2014; **34**: 1163-1177 [PMID: 25208274 DOI: 10.1148/rg.345140190]

42 **Kim EY**, Kwack KS, Cho JH, Lee DH, Yoon SH. Usefulness of dynamic contrast-enhanced MRI in differentiating between septic arthritis and transient synovitis in the hip joint. *AJR Am J Roentgenol* 2012; **198**: 428-433 [PMID: 22268189 DOI: 10.2214/AJR.11.6937]

43 **Thawait SK**, Thawait GK, Frassica FJ, Andreisek G, Carrino JA, Chhabra A. A systematic approach to magnetic resonance imaging evaluation of epiphyseal lesions. *Magn Reson Imaging* 2013; **31**: 418-431 [PMID: 23102949 DOI: 10.1016/j.mri.2012.08.006]

44 **Budzik JF**, Lefebvre G, Forzy G, El Rafei M, Chechin D, Cotten A. Study of proximal femoral bone perfusion with 3D T1 dynamic contrast-enhanced MRI: a feasibility study. *Eur Radiol* 2014; **24**: 3217-3223 [PMID: 25120203 DOI: 10.1007/s00330-014-3340-5]

45 **Bozgeyik Z**, Ozgocmen S, Kocakoc E. Role of diffusion-weighted MRI in the detection of early active sacroiliitis. *AJR Am J Roentgenol* 2008; **191**: 980-986 [PMID: 18806131 DOI: 10.2214/AJR.07.3865]

46 **Sanal HT**, Yilmaz S, Kalyoncu U, Cinar M, Simsek I, Erdem H, Pay S, Dinc A, Tayfun C. Value of DWI in visual assessment of activity of sacroiliitis in longstanding ankylosing spondylitis patients. *Skeletal Radiol* 2013; **42**: 289-293 [PMID: 22740078 DOI: 10.1007/s00256-012-1477-3]

47 **Sahin N**, Hacibeyoglu H, Ince O, Solak A, Uyar B, Erol O, Uslu ZA, Kobak S. Is there a role for DWI in the diagnosis of sacroiliitis based on ASAS criteria? *Int J Clin Exp Med* 2015; **8**: 7544-7552 [PMID: 26221298]

48 **Zhao YH**, Li SL, Liu ZY, Chen X, Zhao XC, Hu SY, Liu ZH, M S YJ, Chan Q, Liang CH. Detection of Active Sacroiliitis with Ankylosing Spondylitis through Intravoxel Incoherent Motion Diffusion-Weighted MR Imaging. *Eur Radiol* 2015; **25**: 2754-2763 [PMID: 25678080 DOI: 10.1007/s00330-015-3634-2]

49 **Zhang M**, Zhou L, Huang N, Zeng H, Liu S, Liu L. Assessment of active and inactive sacroiliitis in patients with ankylosing spondylitis using quantitative dynamic contrast-enhanced MRI. *J Magn Reson Imaging* 2017; **46**: 71-78 [PMID: 27865027 DOI: 10.1002/jmri.25559]

50 **McQueen FM**, Chan E. Insights into rheumatoid arthritis from use of MRI. *Curr Rheumatol Rep* 2014; **16**: 388 [PMID: 24258615 DOI: 10.1007/s11926-013-0388-1]

51 **Nakashima Y**, Tamai M, Kita J, Michitsuji T, Shimizu T, Fukui S, Umeda M, Nishino A, Suzuki T, Horai Y, Okada A, Nishimura T, Koga T, Kawashiri SY, Iwamoto N, Ichinose K, Hirai Y, Arima K, Yamasaki S, Nakamura H, Origuchi T, Takao S, Uetani M, Aoyagi K, Eguchi K, Kawakami A. Magnetic Resonance Imaging Bone Edema at Enrollment Predicts Rapid Radiographic Progression in Patients with Early RA: Results from the Nagasaki University Early Arthritis Cohort. *J Rheumatol* 2016; **43**: 1278-1284 [PMID: 27134251 DOI: 10.3899/jrheum.150988]

52 **Li X**, Liu X, Du X, Ye Z. Diffusion-weighted MR imaging for assessing synovitis of wrist and hand in patients with rheumatoid arthritis: a feasibility study. *Magn Reson Imaging* 2014; **32**: 350-353 [PMID: 24512797 DOI: 10.1016/j.mri.2013.12.008]

53 **Vordenbäumen S**, Schleich C, Lögters T, Sewerin P, Bleck E, Pauly T, Müller-Lutz A, Antoch G, Schneider M, Miese F, Ostendorf B. Dynamic contrast-enhanced magnetic resonance imaging of metacarpophalangeal joints reflects histological signs of synovitis in rheumatoid arthritis. *Arthritis Res Ther* 2014; **16**: 452 [PMID: 25270553 DOI: 10.1186/s13075-014-0452-x]

54 **Sheybani EF**, Khanna G, White AJ, Demertzis JL. Imaging of juvenile idiopathic arthritis: a multimodality approach. *Radiographics*

2013; **33**: 1253-1273 [PMID: 24025923 DOI: 10.1148/rg.335125178]
55 **Rosendahl K.** Juvenile idiopathic arthritis-recent advances. *Pediatr Radiol* 2011; **41** (Suppl 1): 110-112 [DOI: 10.1007/s00247-011-2054-y]
56 **Nusman CM**, Lavini C, Hemke R, Caan MW, Schonenberg-Meinema D, Dolman KM, van Rossum MA, van den Berg JM, Kuijpers TW, Maas M. Dynamic contrast-enhanced magnetic resonance imaging of the wrist in children with juvenile idiopathic arthritis. *Pediatr Radiol* 2017; **47**: 205-213 [PMID: 27957626 DOI: 10.1007/s00247-016-3736-2]
57 **Jans L**, De Coninck T, Wittoek R, Lambrecht V, Huysse W, Verbruggen G, Verstraete K. 3 T DCE-MRI assessment of synovitis of the interphalangeal joints in patients with erosive osteoarthritis for treatment response monitoring. *Skeletal Radiol* 2013; **42**: 255-260 [PMID: 22669732 DOI: 10.1007/s00256-012-1453-y]
58 **Kwok WE**, You Z, Seo G, Lerner A, Totterman S, Ritchlin C, Monu J. High-resolution interleaved water-fat MR imaging of finger joints with chemical-shift elimination. *J Magn Reson Imaging* 2011; **33**: 245-251 [PMID: 21182147 DOI: 10.1002/jmri.22427]
59 **Xu J**, Xie G, Di Y, Bai M, Zhao X. Value of T2-mapping and DWI in the diagnosis of early knee cartilage injury. *J Radiol Case Rep* 2011; **5**: 13-18 [PMID: 22470777 DOI: 10.3941/jrcr.v5i2.515]
60 **Pan J**, Pialat JB, Joseph T, Kuo D, Joseph GB, Nevitt MC, Link TM. Knee cartilage T2 characteristics and evolution in relation to morphologic abnormalities detected at 3-T MR imaging: a longitudinal study of the normal control cohort from the Osteoarthritis Initiative. *Radiology* 2011; **261**: 507-515 [PMID: 21900614 DOI: 10.1148/radiol.11102234]
61 **Baum T**, Joseph GB, Karampinos DC, Jungmann PM, Link TM, Bauer JS. Cartilage and meniscal T2 relaxation time as non-invasive biomarker for knee osteoarthritis and cartilage repair procedures. *Osteoarthritis Cartilage* 2013; **21**: 1474-1484 [PMID: 23896316 DOI: 10.1016/j.joca.2013.07.012]
62 **Gold GE**, Burstein D, Dardzinski B, Lang P, Boada F, Mosher T. MRI of articular cartilage in OA: novel pulse sequences and compositional/functional markers. *Osteoarthritis Cartilage* 2006; **14** Suppl A: A76-A86 [PMID: 16716605 DOI: 10.1016/j.joca.2006.03.010]
63 **Gaspersic N**, Sersa I, Jevtic V, Tomsic M, Praprotnik S. Monitoring ankylosing spondylitis therapy by dynamic contrast-enhanced and diffusion-weighted magnetic resonance imaging. *Skeletal Radiol* 2008; **37**: 123-131 [PMID: 18034343 DOI: 10.1007/s00256-007-0407-2]
64 **Gezmis E**, Donmez FY, Agildere M. Diagnosis of early sacroiliitis in seronegative spondyloarthropathies by DWI and correlation of clinical and laboratory findings with ADC values. *Eur J Radiol* 2013; **82**: 2316-2321 [DOI: 10.1016/j.ejrad.2013.08.032]
65 **Meier R**, Thuermel K, Noël PB, Moog P, Sievert M, Ahari C, Nasirudin RA, Golovko D, Haller B, Ganter C, Wildgruber M, Schaeffeler C, Waldt S, Rummeny EJ. Synovitis in patients with early inflammatory arthritis monitored with quantitative analysis of dynamic contrast-enhanced optical imaging and MR imaging. *Radiology* 2014; **270**: 176-185 [PMID: 23901126 DOI: 10.1148/radiol.13130039]
66 **Cimmino MA**, Innocenti S, Livrone F, Magnaguagno F, Silvestri E, Garlaschi G. Dynamic gadolinium-enhanced magnetic resonance imaging of the wrist in patients with rheumatoid arthritis can discriminate active from inactive disease. *Arthritis Rheum* 2003; **48**: 1207-1213 [PMID: 12746893 DOI: 10.1002/art.10962]
67 **Trattnig S**, Millington SA, Szomolanyi P, Marlovits S. MR imaging of osteochondral grafts and autologous chondrocyte implantation. *Eur Radiol* 2007; **17**: 103-118 [PMID: 16802126 DOI: 10.1007/s00330-006-0333-z]
68 **Wylie JD**, Hartley MK, Kapron AL, Aoki SK, Maak TG. What is the effect of matrices on cartilage repair? A systematic review. *Clin Orthop Relat Res* 2015; **473**: 1673-1682 [PMID: 25604876 DOI: 10.1007/s11999-015-4141-0]

**P- Reviewer:** Ohishi T **S- Editor:** Song XX **L- Editor:** A
**E- Editor:** Lu YJ

Published by **Baishideng Publishing Group Inc**
7901 Stoneridge Drive, Suite 501, Pleasanton, CA 94588, USA
Telephone: +1-925-223-8242
Fax: +1-925-223-8243
E-mail: bpgoffice@wjgnet.com
Help Desk: http://www.f6publishing.com/helpdesk
http://www.wjgnet.com